Antitumor Agents Hot Paper

How to cite: *Angew. Chem. Int. Ed.* **2021**, *60*, 24043–24047
International Edition: doi.org/10.1002/anie.202110041
German Edition: doi.org/10.1002/ange.202110041

In-Cell Generation of Anticancer Phenanthridine Through Bioorthogonal Cyclization in Antitumor Prodrug Development

*Hichem Maslah, Charles Skarbek, Catherine Gourson, Marie-Aude Plamont, Stéphanie Pethe, Ludovic Jullien, Thomas Le Saux, and Raphaël Labruère**

Abstract: *Pharmacological inactivation of antitumor drugs toward healthy cells is a critical factor in prodrug development. Typically, pharmaceutical chemists graft temporary moieties to existing antitumor drugs to reduce their pharmacological activity. Here, we report a platform able to generate the cytotoxic agent by intramolecular cyclization. Using phenanthridines as cytotoxic model compounds, we designed ring-opened biaryl precursors that generated the phenanthridines through bioorthogonal irreversible imination. This reaction was triggered by reactive oxygen species, commonly overproduced in cancer cells, able to convert a vinyl boronate ester function into a ketone that subsequently reacted with a pendant aniline. An inactive precursor was shown to engender a cytotoxic phenanthridine against KB cancer cells. Moreover, the kinetic of cyclization of this prodrug was extremely rapid inside living cells of KB cancer spheroids so as to circumvent drug action.*

In cancer chemotherapy, the prodrug strategy has risen as the cytotoxic drugs available in clinic often present similar toxicity towards both cancer and normal cells. Activity-masked pharmaceuticals activated through enzymatic or chemical reactions by cancer cells were then developed.[1–5] Masked drugs are therefore liberated at the tumor site as a result of modified cancer cell metabolism such as enzymes overexpression, high level of reactive oxygen species (ROS) or hypoxia. The typical prodrug approach consists in branching an organic promoiety to these molecules in order to mask their original activity.[1–6] One major drawback in this prodrug strategy is often the poor ability of the promoiety (regardless of its size) to clearly impair the pharmacological activity of the expected masked drug (e.g. the prodrug can nearly bind as tight as the free drug to the biological target).[7–10]

The enediynes are natural products that cyclize spontaneously into cytotoxic antibiotics.[11–14] Moreover, this scaffold is the sole described as able to afford cytotoxic agents after internal cyclization. Conjugation of these molecules to antibodies lead to the development of the antibody-drug conjugates Mylotarg and Besponsa used in clinic to treat cancer.[15] Furthermore, precursors of coumarins relying on an intramolecular cyclization to eventually generate the fluorophore were also studied.[16–18] Herein, we intend to adapt this feature by establishing chemist-made precursors of antitumor agents operating analogously (Scheme 1 a): 1) no branched organic promoiety is used but masked reactive functions are rather inserted; 2) the proposed prodrug is not a drug linked to a hindered moiety but a synthetic precursor of the drug that will need an in-cell cyclization step to produce the final drug. The prodrug is made of a relatively flexible precursor of the final drug, to strongly reduce the possibility of prodrug potency in respect to the free drug. In this approach, the prodrug displays lower molecular mass in comparison to classic prodrugs, a favorable characteristic for both crossing biological membranes and complying with the Lipinski's rule of 5.

The phenanthridines present large and planar structures which are frequently encountered features of cytotoxic agents. Moreover, phenanthridines are not used in clinic due to their general toxicity,[19–21] and are therefore candidates of choice to explore this strategy. In this context, we prepared ring-opened precursors of phenanthridine designed to target the tumor microenvironment (Scheme 1 b). The prodrugs of phenanthridine contain one masked function, selectively activated into reactive function able to generate the drug by cyclization. The final step of formation of the phenanthridines would be then possible under physiological condition via spontaneous intramolecular cyclization due to entropic favorability as the driving force. Starting from a biaryl precursor, we envisioned a cyclization by imination that would generate the nitrogen-containing central ring of the aromatic phenanthridine. The reactive oxygen species (ROS) overproduction in cancer cells is a common way of anticancer prodrug activation. Indeed, boronic acid precursors are oxidized into corresponding alcohols in the presence of high concentration of hydrogen peroxide or peroxynitrite in cancer cells.[10,22,23] A masked ketone was introduced into our scaffold using a vinyl boronic acid function. In the presence of ROS, the vinyl boronic acid is transformed into an enol moiety tautomerizing into its keto equivalent. The latter group can react with a pendant amine function to build up an imine bond finally shaping the phenanthridine scaffold (Scheme 1 b).

To test our hypothesis, we first prepared a model precursor displaying a scaffold simplified to the maximum as a global proof of concept of our strategy. A convergent synthetic pathway involving an aniline part and a vinyl

[*] H. Maslah, Dr. C. Skarbek, Dr. C. Gourson, Dr. S. Pethe, Dr. R. Labruère
Université Paris-Saclay, CNRS,
Institut de chimie moléculaire et des matériaux d'Orsay
91405 Orsay (France)
E-mail: raphael.labruere@universite-paris-saclay.fr
M.-A. Plamont, Prof. Dr. L. Jullien, Dr. T. Le Saux
PASTEUR, Département de chimie, École normale supérieure
PSL University, Sorbonne Université, CNRS
24, rue Lhomond, 75005 Paris (France)
Supporting information and the ORCID identification number(s) for the author(s) of this article can be found under: https://doi.org/10.1002/anie.202110041.

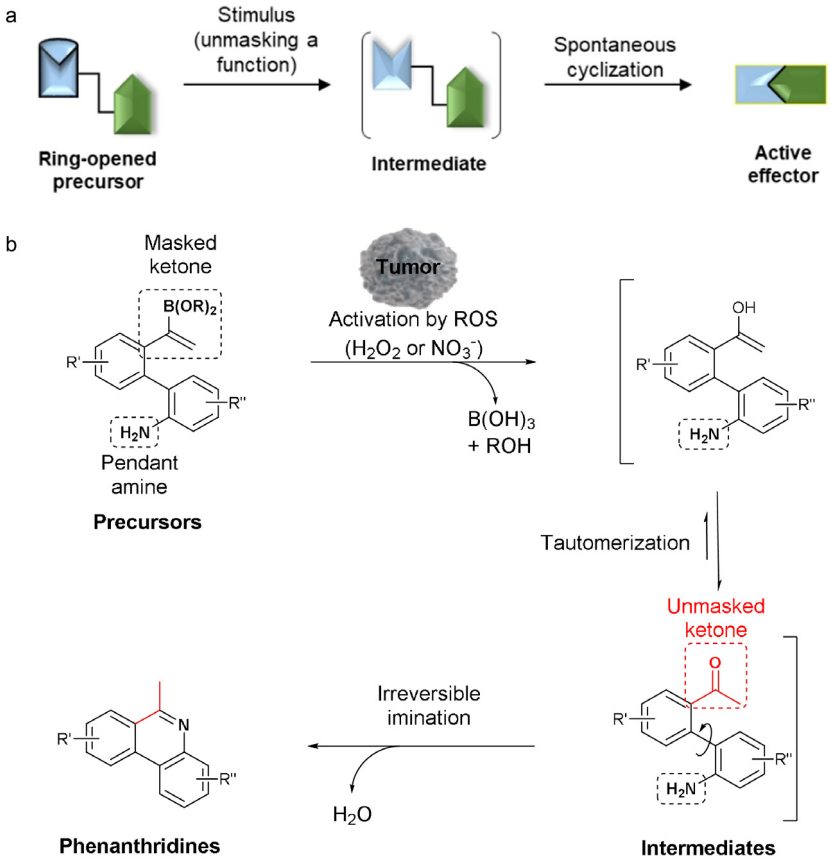

Scheme 1. Generation of anticancer agents from ring-opened precursors through bioorthogonal cyclization. a) Ring-opened antitumor prodrug displaying a spatial structure markedly distinct from the drug is designed to cyclize in cancer cells to finally produce the antitumor drug. Interaction of such prodrug with the biological target is extremely unlikely. b) Vinylboronate precursors expected as pharmacologically inactive will be transformed into the enol intermediate. Subsequent tautomerization will afford the stable unmasked ketone which will undergo spontaneous internal cyclization by imination to form non hydrolysable phenanthridine motifs.

boronate moiety was developed to prepare precursor ProPhen (Scheme 2). This compound was obtained after thorough modulation of the two aryl building-blocks. *N*-Boc aniline (**2a**) was treated with *t*-BuLi leading to an *ortho*-lithiated intermediate which was directly reacted with trimethyltin chloride to afford stannane **3a** in 51% yield. Vinyl boronate **6a** was then prepared in a two-step procedure: (i) starting from iodoacetophenone **4a**, α-boryl alcohol **5a** was obtained in excellent yield using the protocol developed by Hanna et al.[24] involving bis(pinacolato)diboron, 1,3-bis(cyclohexyl)imidazolium tetrafluoroborate ($ICyBF_4$), *t*-BuONa and CuCl; (ii) Subsequent dehydration in presence of *p*-toluenesulfonic acid (PTSA) for 2 hours afforded alkene **6a** in quantitative yield. Formation of biaryl **7a** was achieved via a Stille coupling reaction using $Pd(PPh_3)_4$ and CuCN in toluene heated under reflux. Moreover, we observed a total selectivity for the Stille reaction and no traces of Suzuki homocoupling reaction. Eventually, removal of the Boc protecting group afforded the precursor ProPhen in 45% yield over two steps. In order to study the cyclization of precursor ProPhen, the corresponding product 6-methylphenanthridine Phen of this reaction was prepared through an original synthetic pathway allowing the facile access to phenanthridines (Scheme 3). Starting from anilinostannane **3a** and iodoacetophenone **4b**, we performed four reactions in one-pot: Stille coupling, *N*-Boc deprotection, cyclization by imination and consecutive aromatization. Using this method, we generated variously substituted 6-methylphenanthridines with a view to select the most potent antitumor phenanthridine.

The ability of precursor ProPhen to cyclize was first monitored by ^1H NMR spectroscopy in a mixture of CD_3CN and deuterated PBS buffer (pH 8) using hydrogen peroxide as oxidizing agent triggering the 6-methylphenanthridine Phen formation. By comparing both

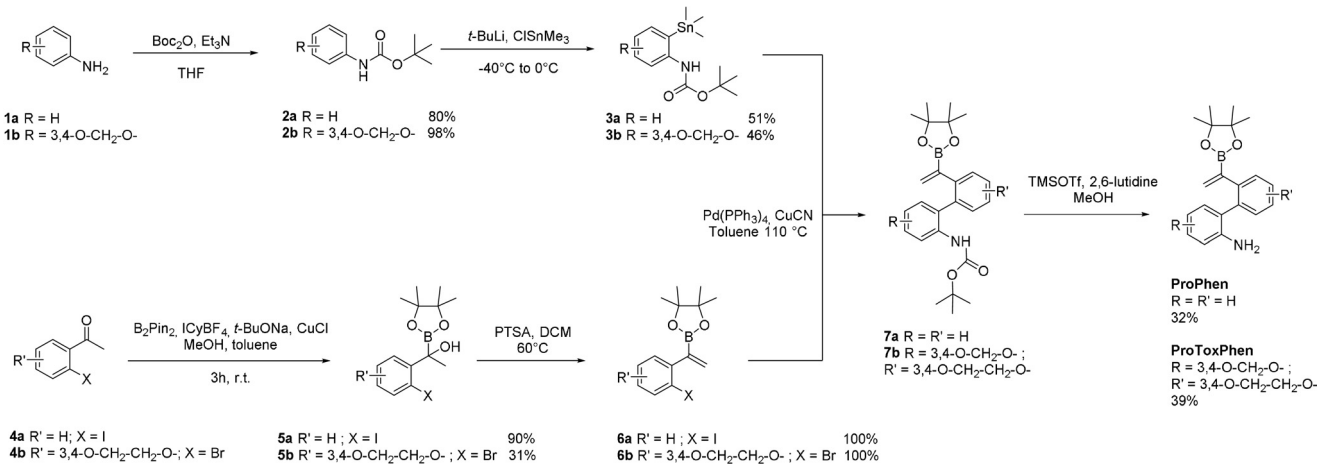

Scheme 2. Synthetic pathway to precursors ProPhen and ProToxPhen.

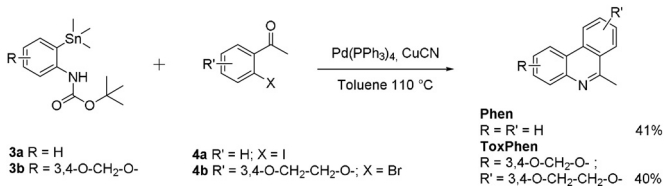

Scheme 3. Synthetic pathway to phenanthridines Phen and ToxPhen.

Table 1: Cytotoxic activity of phenanthridines and biaryl precursors.

Compounds	KB cell viability: 2D [μM]	KB spheroid viability: 3D[a]
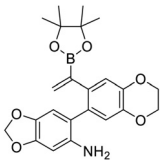	> 500	inactive at 500 μM
ProToxPhen		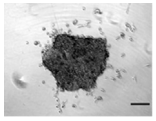
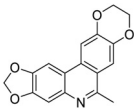	0.7	active at 5 μM
ToxPhen		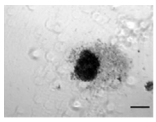

[a] Scale bar: 250 μm.

^{1}H NMR spectra of precursor ProPhen and 6-methylphenanthridine Phen, in particular the disappearance of the gem-hydrogens signal over time, we observed the direct conversion of precursor ProPhen into Phen (Figure S1). Thus, we launched the accurate determination of the kinetic constants of both oxidation and cyclization reactions and, advantageously, phenanthridine Phen is fluorescent as opposed to its precursor ProPhen (Figure S3). We then devised a stopped-flow fluorescence spectrometry experiment to analyze the kinetics of Phen formation initiated by hydrogen peroxide addition to precursor ProPhen. We recorded the temporal evolution of the fluorescence signal from a 0.5 μM solution of precursor in PBS:DMSO 99:1 v:v (pH 7.4) at 25 °C with various H_2O_2 concentrations to rely on a global fit to extract the kinetic constants (Figure S4). Analysis of the experimental data takes into account that phenanthridine Phen generation involves a cascade of reactions as described above (Schemes 1b and S3). As we monitor the steps occurring beyond the millisecond, we reduced the preceding reactive Scheme from three to two steps considering that tautomerization reactions typically occur at the sub-millisecond time scale.[25] In the corresponding reduced Scheme, the rate constant k_1 was associated to oxidation of the C−B bond whereas k_2 refers to the cyclization step (see Scheme S4). Satisfactory fits (see Supporting Information; Figures S4a–c and S5) yielded $k_1 \approx 130\ M^{-1}s^{-1}$. This value indicates a rate of oxidation by hydrogen peroxide of the vinyl boronate ester motif enhanced by a factor 10^2 in comparison with the intensively studied benzene boronate esters (1–2 $M^{-1}s^{-1}$).[26] Then, we extracted $k_2 > 10^2\ s^{-1}$ which represent a time of assembly ($\tau_2 = 1/k_2$) below 10 ms.

Having identified a fast cyclizing scaffold for spontaneous phenanthridine generation, we next examined the feasibility of using such reaction to generate a cytotoxic phenanthridine within tumor tissue. Beforehand, several 6-methylphenanthridines were tested against KB cancer cells (epidermal carcinoma) and polyalkoxyphenanthridine ToxPhen (Table 1 and S1) was selected as the most cytotoxic of this 6-methyl series ($IC_{50} \approx 0.7$ μM, Table S1). The prodrug ProToxPhen of phenanthridine ToxPhen was then prepared (Scheme 2) following the same synthetic pathway devised for unsubstituted precursor ProPhen. The antitumoral activity of the precursors and their corresponding phenanthridines was then evaluated on KB spheroids, a model of in vivo tumors.[27] Both precursors were inactive against KB cells whereas only drug ToxPhen was cytotoxic whether it be in 2D or 3D cultures (Table 1).

Modification of cell and nuclear morphologies induced by our lead compound ToxPhen was then observed by fluorescence microscopy.[28,29] We transfected U2OS cells with H2B-mCherry, a nuclear fluorescent protein marker and further monitored the shape evolution of the nucleus and whole-cell in presence of ToxPhen at different time intervals (Scheme S6). ToxPhen induced several morphological modifications: cell shrinkage, loss of cell-cell contact and nuclear fragmentation which are typical features of apoptosis.

We observed that biaryl prodrug ProToxPhen activity was significantly decreased by a factor superior to 700 ($IC_{50} >$ 500 μM: considered as completely inactive in comparison to the corresponding drug ToxPhen). Such difference of pharmacological activity was expected as ProToxPhen displays a non-planar structure over the completely planar phenanthridine ToxPhen. The dihedral angle of ProToxPhen was then calculated from MM2 energy minimization which afforded 40° (Scheme S5). These data are in agreement with the reported optimal dihedral angle (ca. 43°) obtained on the elementary biphenyl from MP2 calculations.[30] Such twist engenders a significant variation in the 3D structure of the biaryl in comparison to the phenanthridine scaffold.

The faculty of prodrug ProToxPhen to generate the active ToxPhen in a biological context was further evaluated. Interestingly, ToxPhen exhibits suitable fluorescent properties for imaging in living cells (Figure S7). First, we observed that the ester function of ProToxPhen was rapidly hydrolyzed in aqueous media and its boronic acid counterpart was stable in plasma for at least 72 h at 37 °C (See §.7 in Supplementary Information). We further ascertained the quantitative yield of cyclization of ProToxPhen into ToxPhen within KB cells by addition of 50 equivalents of hydrogen peroxide (Figure S8). As no cross reactions were detected in the presence of cells, this ligation by imination can be considered as bioorthogonal in cellulo. Indeed, bioorthogonal reactions are defined by their ability to occur in living systems without hampering the existing biochemical reactions.[31–33] We then achieved the accurate determination of the prodrug conversion kinetics

within KB spheroids. KB cells were incubated for three days in a 150 μM solution of ProToxPhen in DMEM:DMSO 99:1 v:v in order to form observable spheroids. The spheroids were washed with PBS and deposited on a 35 mm glass circular round microscope slide. The prodrug oxidation was then triggered by peroxynitrite, a powerful oxidant of the C–B bond having a physiological half-life ten times higher than that of hydrogen peroxide.[10] To initiate the reaction, a 2 mM solution of peroxynitrite generator 3-morpholinosydnonimine (SIN-1)[34] leading to peroxynitrite production rate of ca. 30 $\mu M\,min^{-1}$ in PBS was added onto the ProToxPhen-containing cells. This continual flux mimics the tumor microenvironment where peroxynitrite production is estimated at ca. 50 $\mu M\,min^{-1}$ essentially supplied by tumor cells and tumor-associated macrophages.[35,36] Considering the rapid decomposition of peroxinitrite in cells (ca. 1.5 s^{-1}),[34] we calculated a steady-state peroxynitrite concentration of ca. 0.3 μM in our experiment. Moreover, peroxynitrite was shown to rapidly diffuse through cell membranes (< 10 ms).[37] Using a homemade epi-fluorescence microscope, we observed ToxPhen fluorescence emission in real time at 440 nm upon illumination at 365 nm (see the Supporting Information and Figure 1).

We first noticed a fast activation-cyclization process into the spheroids going to completion in ca. 5 s. We observed the same cyclization behavior among several cell populations and different spheroids. No cyclization was observed outside the living cells showing the absence of prodrug leakage over the time scale of our experiments. The kinetics of ToxPhen formation within KB cells was analyzed as above. Satisfactory fits (Figure S9) yielded $k_2 > 10^2\ s^{-1}$ in agreement with the value found in vitro. Next, we derived the rate constant of oxidation $k_1 = 1.8\ 10^4\ M^{-1}s^{-1}$ which is 10^2 times faster than the reaction with hydrogen peroxide. A sluggish decrease in fluorescence was subsequently observed as expected from unbalancing production of ToxPhen with its diffusion out of the cells (Figures 1 and S10).

An effective ProToxPhen concentration of 10 μM at the tumor would generate an equal steady-state concentration of ToxPhen at the tumor site in light of the prompt activation-cyclization of the prodrug. This point is fundamental since too long a prodrug conversion would lead diffusion to cause a drop of the drug concentrations at the tumor and its presence far away from the tumor site. Furthermore, the selectivity towards the tumor microenvironment is expected as the production rate of peroxynitrite in healthy cells (ca. 0.1 $\mu M\,min^{-1}$)[35] is 10^2 times slower than the flux found in the pathological condition.

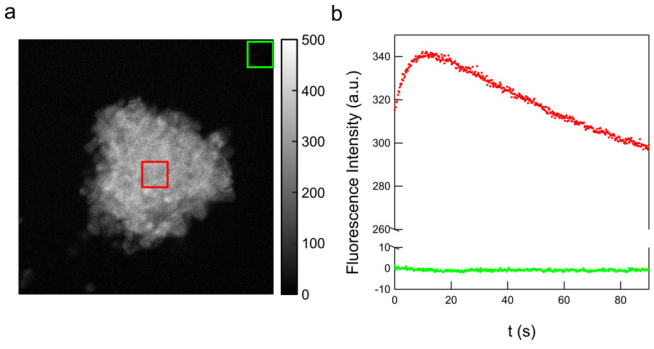

Figure 1. In-spheroid kinetic of cyclisation of ProToxPhen into ToxPhen studied by epifluorescence microscopy. a) Image of the spheroid at time $t = 5$ s after SIN-1 (2 mM) was added to initiate the generation of ToxPhen from ProToxPhen. b) Time evolution of the average fluorescence intensity following the addition of SIN-1. Signal extracted from regions of interest inside (red) and outside (green) the spheroid. Solvent: 100 mM PBS pH 7.4 buffer/DMSO 99:1 (v:v). $T = 37$ °C.

In conclusion, we have described a methodology for the preparation of inactive antitumor prodrugs. These prodrugs were built as ring-opened precursors of the drugs that will cyclize within tumors upon cancer cell-specific stimuli in contrast to the conventional grafting of a bulky temporary moiety hardly inactivating the drug. Using a phenanthridine as drug model and a biaryl precursor able to spontaneously cyclize within tumor spheroid, we demonstrated the feasibility of this strategy. In spite of the presence of a poorly nucleophilic aniline, a fast cyclization of our precursors was measured by virtue of both the geometry of their biaryl scaffolds and the final formation of a six-membered aromatic nucleus. Common imines are rapidly hydrolyzed under physiological conditions and, oxime and hydrazone bonds were introduced to prohibit the reversibility of the former link but these reactions display sluggish kinetics. In this work, the generated imine is inserted in an aromatic ring conferring high stability toward hydrolysis of the newly formed bond. The radically different structures geometry of the prodrug toward that of the drug induced a vast change of cytotoxic activity. New bioorthogonal reactions are constantly investigated in order to either improve existing reactions (i.e. rate constant modifications) or solely access to more complex applications. Thus, this system based on fast cyclization by biorthogonal imination could be expanded to other platforms integrating other types of 1) chemical switch to trigger the reaction and 2) in vivo-compatible synthetic steps. The design of such programed "cycl'in-cell" precursors may find applications in the development of new tools for imaging aside from prodrugs involved in several pathologies.

Acknowledgements

H.M. is supported by the "Ministère de l'Education Nationale de la Recherche et de la Technologie". C.S. is financed by a postdoctoral training grant from the "Fondation ARC pour la recherche sur le cancer".

Conflict of Interest

The authors declare no conflict of interest.

Keywords: Antitumor agents · bioorthogonal chemistry · phenanthridine · prodrug · reactive oxygen species

[1] W. A. Denny, *Eur. J. Med. Chem.* **2001**, *36*, 577–595.
[2] I. Giang, E. L. Boland, G. M. K. Poon, *AAPS J.* **2014**, *16*, 899–913.

[3] X. Zhang, X. Li, Q. You, X. Zhang, *Eur. J. Med. Chem.* **2017**, *139*, 542 – 563.
[4] W. R. Wilson, M. P. Hay, *Nat. Rev. Cancer* **2011**, *11*, 393 – 410.
[5] I.-C. Sun, H. Y. Yoon, D.-K. Lim, K. Kim, *Bioconjugate Chem.* **2020**, *31*, 1012 – 1024.
[6] Y. Singh, M. Palombo, P. J. Sinko, *Curr. Med. Chem.* **2008**, *15*, 1802 – 1826.
[7] R. F. Sherwood, *Adv. Drug Delivery Rev.* **1996**, *22*, 269 – 288.
[8] V. Stella, R. Borchardt, M. Hageman, R. Oliyai, H. Maag, J. Tilley in *Prodrugs: Challenges and Rewards; Biotechnology: Pharmaceutical Aspects*, Springer, New York, **2007**.
[9] W. M. Kavanaugh, *Expert Opin. Biol. Ther.* **2020**, *20*, 163 – 171.
[10] H. Maslah, C. Skarbek, S. Pethe, R. Labruère, *Eur. J. Med. Chem.* **2020**, *207*, 112670.
[11] K. C. Nicolaou, A. L. Smith, E. W. Yue, *Proc. Natl. Acad. Sci. USA* **1993**, *90*, 5881 – 5888.
[12] K. C. Nicolaou, W.-M. Dai, *Angew. Chem. Int. Ed. Engl.* **1991**, *30*, 1387 – 1416; *Angew. Chem.* **1991**, *103*, 1453 – 1481.
[13] A. G. Myers, J. Liang, M. Hammond, P. M. Harrington, Y. Wu, E. Y. Kuo, *J. Am. Chem. Soc.* **1998**, *120*, 5319 – 5320.
[14] A. G. Myers, R. Glatthar, M. Hammond, P. M. Harrington, E. Y. Kuo, J. Liang, S. E. Schaus, Y. Wu, J.-N. Xiang, *J. Am. Chem. Soc.* **2002**, *124*, 5380 – 5401.
[15] A. Adhikari, B. Shen, C. Rader, *Antibody Ther.* **2021**, *4*, 1 – 15.
[16] A. T. Franks, K. J. Franz, *Chem. Commun.* **2014**, *50*, 11317 – 11320.
[17] N. Gagey, M. Emond, P. Neveu, C. Benbrahim, B. Goetz, I. Aujard, J.-B. Baudin, L. Jullien, *Org. Lett.* **2008**, *10*, 2341 – 2344.
[18] N. Gagey, P. Neveu, C. Benbrahim, B. Goetz, I. Aujard, J.-B. Baudin, L. Jullien, *J. Am. Chem. Soc.* **2007**, *129*, 9986 – 9998.
[19] C. Meier, T. N. Steinhauer, F. Koczian, B. Plitzko, K. Jarolim, U. Girreser, S. Braig, D. Marko, A. M. Vollmar, B. Clement, *ChemMedChem* **2017**, *12*, 347 – 352.
[20] W. Feng, M. Satyanarayana, Y.-C. Tsai, A. A. Liu, L. F. Liu, E. J. LaVoie, *Bioorg. Med. Chem.* **2008**, *16*, 8598 – 8606.
[21] L.-M. Tumir, M. R. Stojković, I. Piantanida, *Beilstein J. Org. Chem.* **2014**, *10*, 2930 – 2954.
[22] X. Peng, V. Gandhi, *Ther. Delivery* **2012**, *3*, 823 – 833.
[23] J. Peiró Cadahía, V. Previtali, N. S. Troelsen, M. H. Clausen, *MedChemComm* **2019**, *10*, 1531 – 1549.
[24] R. D. Hanna, Y. Naro, A. Deiters, P. E. Floreancig, *J. Am. Chem. Soc.* **2016**, *138*, 13353 – 13360.
[25] J. Wirz in *Advances in Physical Organic Chemistry* (Ed.: J. P. Richard), Elsevier, Amsterdam, **2010**, *44*, pp. 325 – 356.
[26] N. Rios, L. Piacenza, M. Trujillo, A. Martínez, V. Demicheli, C. Prolo, M. N. Álvarez, G. V. López, R. Radi, *Free Radical Biol. Med.* **2016**, *101*, 284 – 295.
[27] S. Nath, G. R. Devi, *Pharmacol. Ther.* **2016**, *163*, 94 – 108.
[28] C. M. Henry, E. Hollville, S. J. Martin, *Methods* **2013**, *61*, 90 – 97.
[29] H. L. Martin, M. Adams, J. Higgins, J. Bond, E. E. Morrison, S. M. Bell, S. Warriner, A. Nelson, D. C. Tomlinson, *PLOS ONE* **2014**, *9*, e88338.
[30] M. K. Dahlgren, P. Schyman, J. Tirado-Rives, W. L. Jorgensen, *J. Chem. Inf. Model.* **2013**, *53*, 1191 – 1199.
[31] H. C. Hang, C. Yu, D. L. Kato, C. R. Bertozzi, *Proc. Natl. Acad. Sci. USA* **2003**, *100*, 14846 – 14851.
[32] C. R. Bertozzi, *Acc. Chem. Res.* **2011**, *44*, 651 – 653.
[33] J. A. Prescher, C. R. Bertozzi, *Nat. Chem. Biol.* **2005**, *1*, 13 – 21.
[34] F. J. Martin-Romero, Y. Gutiérrez-Martin, F. Henao, C. Gutiérrez-Merino, *J. Fluoresc.* **2004**, *14*, 17 – 23.
[35] C. Szabó, H. Ischiropoulos, R. Radi, *Nat. Rev. Drug Discovery* **2007**, *6*, 662 – 680.
[36] X. Lin, W. Zheng, J. Liu, Y. Zhang, H. Qin, H. Wu, B. Xue, Y. Lu, P. Shen, *Antioxid. Redox Signaling* **2013**, *19*, 1337 – 1355.
[37] A. Denicola, J. M. Souza, R. Radi, *Proc. Natl. Acad. Sci. USA* **1998**, *95*, 3566 – 3571.

Manuscript received: July 27, 2021
Revised manuscript received: August 26, 2021
Accepted manuscript online: September 6, 2021
Version of record online: October 5, 2021

